ACS Photonics

Article

Cite This: ACS Photonics 2019, 6, 1425−1433

pubs.acs.org/journal/apchd5

Open-Type SPP Waveguide with Ultrahigh Bandwidth up to 3.5 THz

Pavel N. Melentiev,*[,†,‡] Alexey Kalmykov,[†,‡] Arthur Kuzin,[†,§] Dmitriy Negrov,[§] Vasiliy Klimov,[∥,⊥] and Victor I. Balykin[†,‡]

[†]Institute of Spectroscopy Russian Academy of Sciences, Phizicheskaya str., 5, Troitsk, Moscow 108840 Russia

[‡]National Research University, Higher School of Economics, Moscow 101000, Russia

[§]Moscow Institute of Physics and Technology, Moscow reg., Dolgoprudny, 141700, Russia

[∥]National Research Nuclear University MEPhI, Kashirskoe shosse, 31, Moscow 115409, Russia

[⊥]P.N. Lebedev Physical Institute of the Russian Academy of Sciences, Leninsky Prospekt, 53, Moscow 119991, Russia

Supporting Information

ABSTRACT: Due to losses in metals, the propagation length of the surface plasmon-polariton (SPP) waves on metal surfaces is small. This severely limits development of numerous applications of the SPP optics: in the near-infrared spectral region propagation length of SPP waves is no longer than 200 μm as for plane SPP waves and for all types of SPP waveguides. In this work, we show that the focusing of SPPs allows for the first time realizing open-type waveguide for SPP waves characterized by long distance of SPP effective propagation length up to 1 mm at a wavelength of 780 nm. We show that focused SPP waves in such a waveguide can be effectively excited by a 16 fs laser as well as be amplitude modulated within a bandwidth about 3.5 THz. The fast dynamics of the focused SPP waves is limited by the SPP group velocity dispersion. The large effective propagation length of the SPPs and its ultrahigh bandwidth open up new possibilities for using focused SPPs in different areas of plasmonics and photonics.

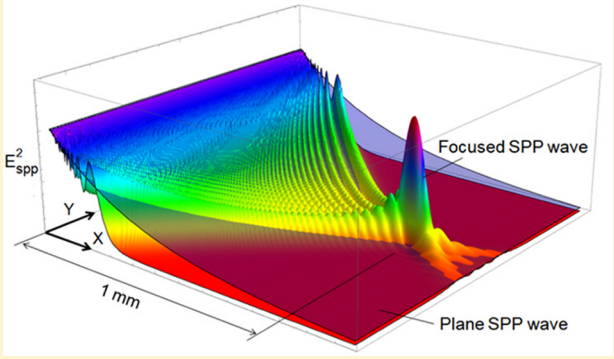

KEYWORDS: *plasmonics, NIR plasmonics, SPP on Ag films, long propagating SPP, SPP focusing, highspeed interconnects*

The integration of electronic and optical circuits is constrained by the dimensions mismatch of their elements.[1−3] Elements of electronic circuits can be manufactured with sizes less than 30 nm. The typical wavelength of light used in photonics schemes has a value of about 1 μm. Integration of electronic and optical circuits is possible on the basis of the use of surface plasmon-polariton (SPP) waves in metallic nanostructures that allows simultaneous transfer of optical and electrical signals through the same metal elements, thereby creating the opportunity to realize the technical advantages of photonics and electronics on a single chip.

Methods of SPP waves control are developing within the framework of plasmon optics, one of the existing types of optics (photon optics, atom optics, and optics of charged particles). In plasmon optics, the propagation and control of SPP waves parameters is investigated, as well as the development of its various elements: lenses, mirrors, waveguides, lasers, sensors, and so on.[4,5] Unfortunately, media for SPP waves excitation (metal surfaces) are characterized by large losses,[6] which greatly differs plasmon optics from other types of optics, where the propagation of the corresponding waves occurs over considerably longer distances and can be practically unlimited. Thus, the record length of SPP waves propagation on the surface of the silver film is about 200 μm (for the SPP wavelength at 780 nm) and was demonstrated on a single-crystal silver film.[7] The short SPP propagation lengths lead to short SPP lifetimes, as well as to various limitations to the fabrication of optical circuits using SPP (geometric dimensions, edge effects, parasitic light background, etc.). When using polycrystalline films, the problem becomes even more serious, because of the significantly shorter propagation lengths of SPP waves.[8]

There are only two ways to increase the SPP propagation length. One such approach is to create conditions under which SPP waves propagate predominantly in the lossless dielectric media in such a way that only a small part of the SPP field is located within the metal. An example is the use of one-dimensional photonic crystals as a dielectric media adjacent to a metal film surface that leads to a considerable decrease of the SPP losses in metal, and as a result, increasing the SPP propagation length to a record high value about 0.8 mm (at SPP wavelength about 715 nm).[9] However, this approach uses high quality ultrathin metal films (about 20 nm thick) and one-dimensional photonic crystals, both having diffculties in their technical realization as well as the complexity of their practical use.

Received: December 28, 2018
Published: May 15, 2019

Downloaded via NOTTINGHAM TRENT UNIV on July 29, 2019 at 20:33:39 (UTC).
See https://pubs.acs.org/sharingguidelines for options on how to legitimately share published articles.

© 2019 American Chemical Society

DOI: 10.1021/acsphotonics.8b01787
ACS Photonics 2019, 6, 1425−1433

Another approach of increasing the SPP propagation length is the active compensation of SPP waves losses with a use of an active medium (dye molecules, quantum dots, heterostructures) deposited on the surface of metal films.[10,11] The active medium is pumped by a laser radiation or current and can transfer energy to the SPP wave excited on the metal film surface. In practice, it is even possible to fully compensate SPP losses, which results in the SPP lasing.[12−14] The disadvantages of this approach are the complexity of the technical implementation, the use of additional expensive equipment for pumping the active medium, high sample heating caused by the active medium pumping, temporal degradation of the active medium, and strong parasitic background caused by the luminescence of the active medium.

The long SPP propagation length is important for the development of the key element of integrated plasmonics: a plasmonic waveguide.[15,16] Characteristic features of plasmonic waveguides are (i) the possibility of achieving subwavelength transverse localization of the guided mode field and (ii) substantial ohmic losses in metal parts of the waveguide leading to a decrease in the propagation length. For plasmonic waveguides of all types, an increase in the degree of the guided mode field transverse localization leads to a decrease in the mode propagation length.[16−19] With an increase in the degree of transverse localization of the mode, the field penetrates deeper into the metal parts of the waveguide, leading to an increase of ohmic losses. There are many types of SPP waveguides developed: slit-based,[20] groove-type,[21] wedge-type,[22] dielectric-loaded,[23,24] and many others.[25−30] But today, for all types of waveguides, the SPP propagation lengths are smaller than the plane SPP wave propagation length and do not exceed 100 μm in the near-infrared spectral region.[26]

Another important application of long propagating SPP waves is its use for ultrasensitive detection, connected with realizing long interaction lengths of SPPs with analyte molecules having absorption at SPP wave frequency.[31,32] In such applications the analyte molecules are arranged on a way of SPP propagation. Absorption of SPP waves by analyte molecules, long interaction length, and measurement of SPP absorption by analyte molecules can help to reach ultimate sensitivity in analogy with conventional spectroscopy techniques.[14]

The open-type resonators are quite common in a modern electrogynamics and particular in laser physics today. But exactly the concept of the open-type resonators finally led to achieving the first demonstration of laser. In the simplest case, the open resonator consists of two mirrors located opposite to each other. Such systems were almost simultaneously suggested by Prokhorov,[33] Shavlov, and Townes.[34] This is the first, but not the last, application of open resonators and waveguides. The open resonators are remarkable by the fact that all their dimensions are much larger than the light wavelength, but the spectrum of their own frequencies is not so dense compared to the spectrum of closed resonators of the same dimensions. At the same time, the diffraction and other radiation losses of some modes of an open resonator can be made very small, so that these modes have high Q-factors, often exceeding the Q-factors of modes in closed resonators.

There are information transmission lines based on the same principles as open resonators: "open-type waveguides". In the cross section of such waveguides the field is not limited by any impenetrable walls (as in a conventional waveguides). These lines use optical elements: lenses or mirrors. Open waveguides formed by periodically placed lenses have been proposed in the work.[35] When passing through such a waveguide, the light periodically focuses and defocuses by the lenses. The multiple focusing and defocusing help compensating diffraction losses, known as a main limiting factor of long distance information transfer with use of a freely propagating light waves. Various open-type waveguide geometries and the relationship between open waveguide theory and open resonator theory are discussed in a book.[36]

In this work, we propose a new method for SPP waveguiding due to its focusing over a long distance, far exceeding the length of a freely propagating plane SPP wave. Note that SPP wave focusing was already realized using the structuring of the surface of a metal film by curved ridges,[37] curved slits,[38,39] curved chain of nanoparticles,[40] by creating a dielectric lens on the metal film, in a direct analogy with photon optics[41] or with use of multiple focusing elements.[42] The main purpose of focusing considered in the current work is to dramatically minimize the lost of information carried out by SPP waves on long distance, associated with losses of SPP in metals as well as due to a diffraction of SPP waves. With such focusing, we demonstrate for the first time in plasmonics the open-type waveguide. This approach allows us to significantly increase the local intensity of the SPP wave along the direction of its focusing and, thus, significantly increase the "effective" propagation length of the SPP wave.

FIELD DISTRIBUTION OF SPP WAVES IN THE OPEN-TYPE SPP WAVEGUIDE

Figure 1 shows the geometry of the SPP open-type waveguide, the SPP excitation and detection studied in this work. The SPP

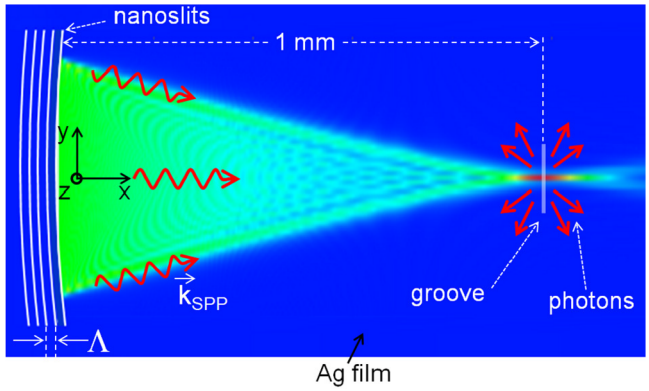

Figure 1. Geometry of the open-type SPP waveguide formed by an array of nanoslits in the shape of an arc (X and Y dimensions are not to scale). The spatial intensity distribution of the focused SPP wave is shown as a background.

propagates on a surface of a 100 nm thick Ag film deposited on a quartz substrate. The SPP is excited with an array of slits in the Ag nanofilm with a period Λ = 780 nm. The slits are illuminated by a laser radiation with a wavelength around 780 nm (the wavelength was fine-tuned to maximize effciency of the SPP excitation) from the side of the quartz substrate and perpendicular to the substrate surface. At the chosen parameters of the nanoslits array and the chosen laser light wavelength, the efficiency of converting the laser light into a SPP wave up to 6% can be achieved:[38] rather high coupling efficiency, approaching the coupling efficiencies of SPP waveguides in a less lossy 1.5 μm spectral range.[43−47] The

DOI: 10.1021/acsphotonics.8b01787
ACS Photonics 2019, 6, 1425−1433

slits have a shape of an arc of radius R_0 = 1 mm and the shape of the slits makes it possible to focus the SPP wave into a diffraction-limited spot.[38] To detect the SPP focusing and the SPP effective propagation length a nanogroove is arranged in the region of the geometric focus of the nanoslits array. As we will show below, the far-field measurements of the SPP scattering on the nanogroove allows one to measure the effective SPP propagation length as well as SPP dynamics (Figure 1).

The chosen geometry of the SPP wave formation has a number of significant advantages. First, focusing allows increasing the intensity of the SPP field along a propagation line (compared to a plane SPP wave) and in the focus region, which, as will be shown below, may be rather far from the excitation region of the SPP wave. Since the local SPP intensity is considered (the SPP intensity along the focused SPP wave propagation line), it seems reasonable to introduce the "effective" propagation length L_{eff}. In open-type SPP waveguide, the "effective" propagation length roughly equals focusing distance of a converging SPP wave. The "effective" propagation length of focused SPP waves can be much larger than the plane SPP waves propagation length on the Ag film surface. In addition, the small transverse size of the SPP in the focal region allows a significant increase in the signal-to-noise ratio when registering the focused SPP waves. This allows registering low intensity SPP signal against the background of a large parasitic signal from the exciting laser radiation.

The transverse localization of the SPP wave in open-type SPP waveguide is determined by two parameters: (1) the size of nanoslits exciting SPP waves having a transverse size of about 50−100 μm, and (2) the transverse size of SPP wave in focus having a value of about 2−5 μm. Moderate transverse localization of SPP waves is a typical characteristic for all open-type waveguides. As it is well-known in optics, the characteristic values of the transverse localization in open-type waveguides are determined by the technology of manufacturing mirrors, as well as by the existing diffraction constraints.[48,49]

To calculate the SPP focusing and propagation, we consider the SPP excitation by a system of point sources of equal intensity uniformly distributed along an arc of radius R_0 and with a central angle $2\theta = \pi/19$. We calculated the distribution of electromagnetic field of the excited SPP[50] using the Wolfram Research Mathematica package (see Supporting Information for details). Figure 1 presents the 2D distribution of the SPP intensity close to the Ag nanofilm surface, when the SPP is excited by point sources of equal intensity distributed along the arc of the radius R_0. As can be seen from the figure, the SPP wave is focused to the geometric center of the arc. The calculation was carried out for the case of small SPP losses being four times smaller than the measured value for SPP losses of Ag film used in measurements presented below.

Figure 2 shows the calculated intensity distribution of the focused SPP wave as a function of its propagation distance, with the SPP losses taken from our measurements. The measured SPP propagation distance on a 100 nm thick Ag film that was used in our experiments equals 125 μm at the excitation wavelength of 780 nm. The figure shows the intensity distribution of the SPP excited by a system of point sources arranged on the Ag nanofilm surface along the arc of radius R_0 as a function of the distance to the point sources. The sources have equal intensity and are uniformly distributed along an arc. The SPP intensity distribution is shown along the

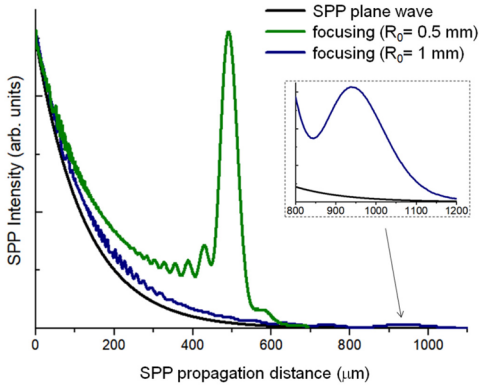

Figure 2. Intensity distribution of the SPP wave excited by a system of point sources arranged along the arc of radius R_0 as a function of the distance to the point sources. The intensity distributions are shown along the symmetry line (axis x, see Figure 1) for three cases: (1) the excitation of a plane SPP wave by point sources arranged along a straight line (black curve), $R_0 = \infty$; (2) the excitation by point sources located on the arc, with R_0 = 0.5 mm (green curve); (3) the excitation by point sources located on the arc, with R_0 = 1 mm (blue curve). The inset shows the SPP intensity dependence in the focal region for R_0 = 1 mm.

focused SPP propagation line (axis x, see Figure 1) for the three cases: (1) the excitation by point sources arranged along a straight line, $R_0 = \infty$ (black curve), (2) the excitation by point sources located on the arc with R_0 = 0.5 mm (green curve), and (3) the excitation by point sources located on the arc, with R_0 = 1 mm (blue curve). The inset in the figure shows the dependence in the focal region for the case of R_0 = 1 mm. For all three cases, the power of the SPP wave was chosen to be the same for all geometries.

As can be seen from Figure 2, in the case of the plane SPP wave (black curve), the intensity decays exponentially at a length of 125 μm ($1/e$), and there is no focusing. When the SPP wave is excited by a system of point sources located along an arc with a radius R_0 = 0.5 mm (green color), one can see the pronounced focusing. Indeed, an Airy pattern of the focused SPP wave is seen at a distance of 480 μm from the excitation line. The Airy pattern length equals 100 μm. A strong increase in the SPP wave intensity is observed in the focal region. A similar pattern is observed when SPP is excited by a system of point sources located on the arc with R_0 = 1 mm (blue curve). The focused SPP wave is visible at a distance of 940 μm from the excitation line. The Airy pattern length is about 200 μm.

For both cases of SPP wave focusing (Figure 2), the region of SPP focusing does not coincide exactly with the geometric focus determined by the arc radius. Focusing of the SPP occurs at distances smaller than the corresponding arc radii. This happens due to the losses of the SPP wave. If these losses are negligible, then SPP focusing is observed directly in the geometric focus (see Figure 1). Strong SPP losses lead to a noticeable shift in the position of the SPP intensity maximum. We note that the Airy pattern length in the case of arc having radius R_0 = 1 mm is twice larger in comparison with an arc having radius R_0 = 0.5 mm due to a 2-fold decrease in the convergence angle of the SPP wave in the chosen geometry of SPP wave excitation.

SPP focusing allows us to compensate the decrease of the local intensity of SPP waves as they propagate. As can be seen from Figure 2, for the case of focusing with R_0 = 1 mm, the intensity in the focal point is approximately 80 times smaller

DOI: 10.1021/acsphotonics.8b01787
ACS Photonics 2019, 6, 1425−1433

than the intensity near the SPP excitation region. Nevertheless, the SPP intensity in the focus is approximately 25× larger than the intensity of the plane SPP wave (see the inset in Figure 2).

An important characteristic of the open-type SPP waveguide is the value of the intensity of SPP wave in focus region. The intensity depends on several factors: (1) losses of SPP waves in metallic film, the larger the focusing distance R_0, the larger the losses; (2) SPP waves local intensity increase due to its focusing; (3) transversal size of the SPP in a focal spot, determined by diffraction constraints. Figure 3 shows the

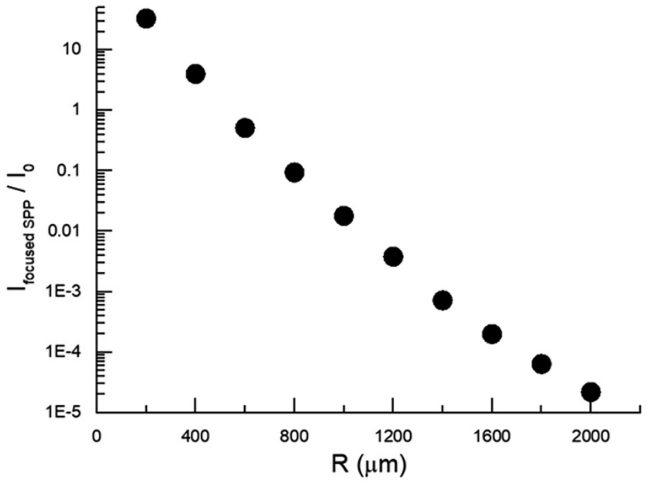

Figure 3. Calculated values of maximum intensities of focused SPP wave in a focus area for open-type SPP waveguides having different arc radius R_0 values.

calculated values $I_{focused\ SPP}$ of the SPP wave amplitude in its focus area in the open-type SPP waveguide, depending on the focus value R_0. As it is seen from the figure, at small focus values R_0 < 500 μm, corresponding intensities of the SPP waves in the focus can even exceed the intensity of SPP waves in its excitation region I_0. This regime of focusing was recently explored to reach high values of SPP local intensity.[38] Long distance focusing corresponds to an open-type SPP waveguiding regime. As it is seen from Figure 3, at a focusing distance of about 1 mm, the $I_{focused\ SPP}/I_0$ value equals 1.8%, enough value for effective registration of the SPP waves. This regime of focusing will be used below to build open-type SPP waveguide.

EXCITATION AND DETECTION OF SPP WAVES IN OPEN-TYPE SPP WAVEGUIDE

To excite SPP waves in open-type SPP waveguide an array of nanoslits forming the waveguide was irradiated by laser radiation having linear polarization along the x axis (see Figure 1). As a source of laser radiation, a titanium−sapphire tunable laser was used. The laser spot on the array of nanoslits had a size of 15 μm × 80 μm. Optical measurements were performed using an inverted Nikon Ti/U microscope equipped with a 2D CCD camera (Princeton Instruments, PhotonMax model).

To verify focusing of SPP waves in an open-type SPP waveguide, we used an approach of the so-called optical microscopy of SPP waves with use of plasmonic nanostructures.[7,38] For that purpose, in an open-type SPP waveguide we arranged an array of nanogroove detectors directly in a way of converged SPP waves propagation. The excited SPP waves are partially scattered on these nanogrooves, thus, forming corresponding far-field optical image of the SPP wave propagation. Experimental sample of an open-type SPP waveguide having nanogroove detectors was built on a polycrystalline 100 nm thick Ag nanofilm. The measured SPP propagation length is about 125 μm at an excitation wavelength of 780 nm. The propagation length was measured by the optical microscopy of SPP waves.[38] To excite and focus SPP waves, we fabricated on the Ag nanofilm surface using a focus-ion-beam milling method an array of seven nanoslits having a shape of an arc of radius R_0 = 1 mm, with a spatial period of 780 nm and the arc length of 47 μm. Along the way of converged SPP wave propagation, an array of nanoslits having size 120 nm × 47 μm were fabricated. Note that the Ga ion beam provides not only milling, but also diffusion of Ga ions into the Ag film, leading to additional SPP losses.[51] The use of other types of lithography (based on the use of He or Au ion beams) can lead to better sample quality.

Figure 4a shows both types of nanostructures. One is the array of nanoslits (first vertical thick gray line from the left),

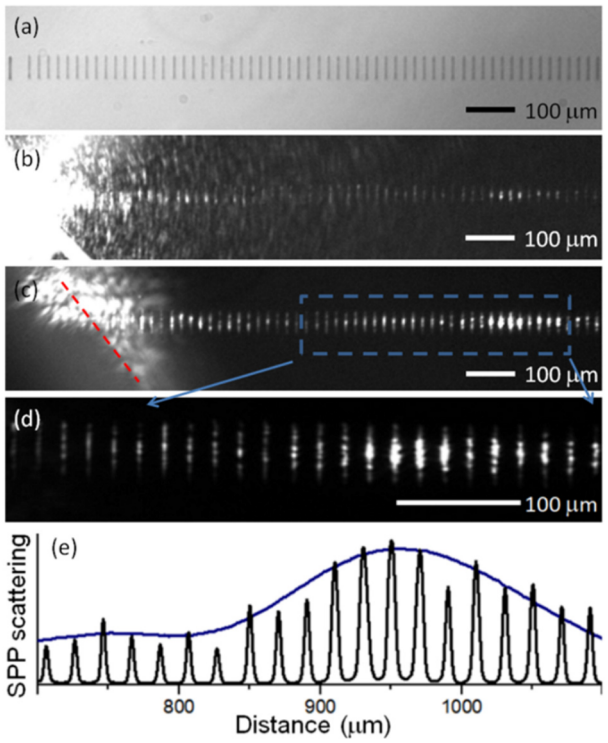

Figure 4. Excitation and detection of SPP waves in open-type SPP waveguide: optical image of experimental sample under a white-light illumination (a), detection of SPP waves excited by 780 nm laser light (b), the same optical image obtained with the use of a shield to block laser light passed through the slits (edge of the slit is shown by red hatched line) (c), and an optical image obtained with a higher magnification rate of optical microscope objective (d). (e) The black line shows a cross-section of image (d) and the blue curve shows the results of the corresponding calculations.

designed to excite convergent SPP waves. The distance between nanoslits is too small to be resolved by the optical microscope. The figure also shows distinctly separated nanogroove detectors. These nanogrooves are arranged parallel to the nanoslits and are on the way of the SPPs propagation.

DOI: 10.1021/acsphotonics.8b01787
ACS Photonics 2019, 6, 1425−1433

Figure 4b shows the optical image of an experimental sample shown on Figure 4a when it is irradiated by laser radiation at wavelength 780 nm. As it can be seen from the figure, the strong scattering of laser radiation on the array of nanoslits and the excitation of convergent SPP waves on the Ag film surface appear. The convergent SPP waves propagate and scatter on nanogrooves, giving the possibility to visualize SPP propagation in an optical microscope. Each of the spots on a nanogroove has an elliptical shape. The smaller diameter of this spot is determined by a diffraction limitation of optical objective used. The larger diameter of the spot is determined by transversal size of convergent SPP waves and a length of nanogrooves (47 μm). When SPP wave transverse size is larger than nanogroove length, then the corresponding spot size equals 47 μm. In the opposite case, when the SPP wave transverse size is smaller than a nanogroove length, then the corresponding spot size is equal to the SPP size. Both cases are seen in the figure. The important point is that the focal spot of the SPP wave is clearly seen: nanogrooves located in the region of the SPP focusing are seen much brighter than neighboring nanogrooves. The Airy pattern length of focused SPP waves measured in such a way equals about 200 μm and are located at a distance of about 1 mm from the excitation region.

Figure 4b clearly demonstrates one of the important advantages of an open-type SPP waveguide: focused SPP wave is seen even at a very high background formed by scattering of the excitation laser radiation. This is a consequence of long distance focusing of the SPP wave that helps to arrange the SPP detection region 1 mm distance from the SPP excitation region.

To eliminate unwanted scattering formed by exciting the laser radiation, we used a nontransparent opaque shield that we place 0.5 mm close and parallel to the sample. Figure 4c shows an optical image obtained with the same experimental condition as presented in Figure 4b, but with the shield installed (edge of the slit is indicated by red hatched line). As it is seen from the figure, the shield blocks most of the laser light passed through the excitation slits and helps dramatically improve the signal-to-noise ratio in the optical image. Thus, in Figure 4c, the focusing of convergent SPP waves is seen to be even more profound. To see the region of SPP focusing in more details, we changed the microscope optical objective on another one having a higher magnification factor. The resulting image is presented on Figure 4d. This figure shows not only focusing of SPP waves, but also details of SPP scattering on each individual nanogroove: image of every nanogroove has small bright spots. It is a well-known feature that is related to enhanced scattering of SPP waves on Ag nanocrystals. Indeed, due to the polycrystalline structure of the Ag film, every nanogroove has a corresponding roughness on its edges, forming hot spots of SPP wave scattering.

Figure 5 shows the optical image of a nanogroove located in the focal region (exactly 1 mm far from the SPP excitation region) of the open-type SPP waveguide sample when the SPP wave is excited. The measurements were made with two different mutually perpendicular polarizations of the laser light (Figure 5a,b). If the laser light polarization is chosen parallel to the y-axis, then the SPP excitation efficiency becomes extremely low and, as a consequence, the SPP focusing is not observed in Figure 5a. On the contrary, at the laser light polarization along the x-axis, there is an efficient SPP wave excitation, and a bright spot corresponding to the focused SPP wave scattering on the nanogroove is observed in Figure 5b.

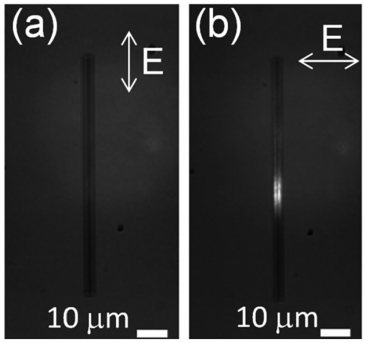

Figure 5. Scattering of a focused SPP on a nanogroove located in the SPP focusing area: optical images of the nanogoove area of open SPP waveguide sample at a different polarizations of excitation laser radiation: (a) E-field is aligned along the groove; (b) E-field is aligned perpendicular to the groove.

Our theoretical estimations show that the ratio of intensities in focus for different polarizations is about 27 (see Supporting Information for details).

At the chosen geometry of open-type SPP waveguide, a convergence angle of the SPP wave equals $2\theta = 2.6°$. Thus, the diffraction limited lateral size of the SPP wave at the focus is $\Delta y = \lambda/2 \sin \theta = 17.6$ μm. As can be seen in Figure 5b, the lateral size of the SPP wave on the nanogroove is 20 μm, which is just sligthly larger than the calculated value (see above). The main reason for that is due to the fact that the nanogroove is arranged not exactly at the position of the SPP focusing spot (see above). Note another factor may increase the SPP wave lateral size in the focus. In calculations it was assumed that the intensity of point sources is the same over the entire arc. While in a real experiment the spatial distribution of the intensity of the laser spot is close to the Gaussian form and, therefore, the laser intensity on the nanoslits vary along the nanoslits, leading to nonuniform excitation of the SPP wave. Another factor is that the angle between the polarization of the laser light and the nanoslits also varies along the nanoslits, also making an impact on the nonuniform SPP excitation along the nanoslits. In addition, in the "nanogroove-detector", excitation of the metal−dielectric−metal (MDM) SPP mode[52] is possible, which may lead to an additional increase in the lateral size of the SPP wave on the nanogroove.

ULTRAFAST DYNAMICS OF THE SPP WAVE IN AN OPEN-TYPE SPP WAVEGUIDE

The focusing of SPPs allows a significant increase in the SPP effective propagation length, and this made it possible to consider the open-type SPP waveguide as a plasmonic interconnect line. In direct analogy to photon optics, the amplitude modulation bandwidth of a focused SPP wave is determined by the group velocity dispersion of the SPP wave spectral components. This means that due to the SPP group velocity dispersion, the duration of a short SPP pulse increases as it propagates.[53] Indeed, after the SPP pulse propagation of length L there will be an increase in the duration of the pulse of the SPP wave by the following amount: $\Delta t_{SPP} = L\Delta v_{gr}/v_{gr}^2$, where Δv_{gr} is the change in the width of the group velocity of the SPP pulse.

Our estimates based on the measured SPP group velocity dispersion data show that, at the excitation wavelength of about 780 nm, the SPP group velocity dispersion at the length

DOI: 10.1021/acsphotonics.8b01787
ACS Photonics 2019, 6, 1425−1433

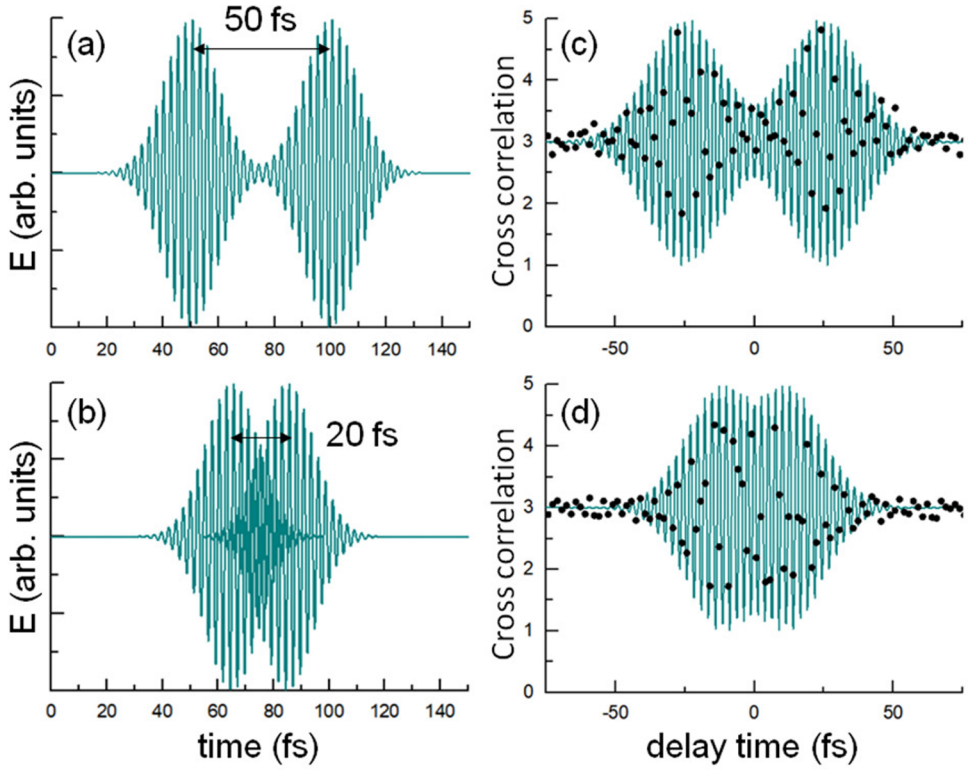

Figure 6. Results of measured and calculated cross-correlation functions. SPP pulses in an open-type SPP waveguide are excited by three laser pulses of 16 fs duration. The time delay between $E_1(t)$ and $E_2(t)$ equals to 50 fs (a,c) and 20 fs (b,d). The third pulse has a variable delay τ: $E_3(t - \tau)$. (a, b) Time dependence of the field for a pair of laser pulses $E_1(t)$ and $E_2(t)$; (c, d) Measured (black dots) and calculated (lines) cross-correlation functions of the first order for SPP waves excited by pulses $E_1(t)$, $E_2(t)$, and $E_3(t - \tau)$.

L = 1 mm leads to additional broadening of the SPP pulse to a value about 15 fs (see Supporting Information for details).

To study ultrafast dynamics of the open-type SPP waveguide, we performed the measurements of SPP focusing at the excitation of our sample by a pair of laser pulses $E_1(t)$ and $E_2(t)$, with a variable delay between these pulses. Measurements of the SPP interconnect line bandwidth was carried out using the cross-correlation technique (see Supporting Information for details). For that purpose, a laser pulse of 16 fs duration was passed through a doubled Michelson interferometer formed by three 100% mirrors and two 50/50 beam splitters (see Supporting Information for details). Such an interferometer allows the laser pulse to be divided into three pulses of the same amplitude: $E_1(t)$, $E_2(t)$, and $E_3(t)$. The delay between these pulses is determined by the corresponding length of the interferometer arms.

Each laser pulse $E_i(t)$ excites the SPP pulse E_i^{SPP} in open-type SPP waveguide. The cross-correlation function is measured by a change of the third pulse delay τ (see Supporting Information for details):

$$F_1^{SPP}(\tau) \sim \int_{-\infty}^{+\infty} [E_1^{SPP}(t) + E_2^{SPP}(t) + E_3^{SPP}(t)(t - \tau)]^2 dt$$

To measure the ultrafast dynamics, we excited the open-type SPP waveguide by femtosecond laser pulses (16 fs pulse duration) having a central frequency at 780 nm (see Supporting Information for details). For the 16 fs Fourier-limited laser pulses, the corresponding spectral width is about 60 nm.

A large spectral width of laser pulses imposes fundamental physical limitations on the femtosecond SPP pulse excitations. The SPP excitation by an array of nanoslits, as shown in Figure 1, helps to realize a high coupling rate of laser light to SPP wave. This is due to the constructive interference of SPP waves excited by laser radiation on each nanoslit. However, the passage time of SPP waves between two nanoslits lies in the femtosecond time range. This leads to a large increase in the SPP pulse duration. In order to produce a femtosecond SPP pulse with duration about the laser pulse duration we used a modified scheme of SPP excitation: instead of using the nanoslits array the SPP excitation is realized with a single nanoslit in the shape of an arc having radius R_0 = 1 mm (exactly like it was considered in our simulations of a focused SPP waves intensity distributions presented above). In the geometrical in the focal region of this arc we fabricated a nanogroove for the detection of the focused SPP pulses in a direct analogy of the scheme presented on Figure 1.

In a separate experiment, we measured spectrum of focused SPP waves excited by a 16 fs laser pulses. For that purpose, we measured spectrum of radiation emitted from the nanogroove caused by the focused SPP wave scattering excited by the 16 fs laser pulses. Our measurements show that this spectrum is almost identical to the spectrum of the laser radiation with a spectral width equal to 60 nm (see Supporting Information for details). In others words, the SPP excitation efficiency is almost the same for all spectral components of the laser light. This is an important characteristic of the extra-long SPP waves focusing that shows that it is possible to excite long distance propagating focused SPPs waves having all spectral components to form SPP wave pulse having femtosecond time duration, almost the same as the excitation laser pulses have.

DOI: 10.1021/acsphotonics.8b01787
ACS Photonics 2019, 6, 1425−1433

Figure 6a,b shows the temporal dynamics of two 16 fs pulses with a delay between pulses which equals 50 and 20 fs, respectively. As can be seen from the figures, both pulses are clearly distinguishable at a delay between pulses equal to 50 fs. Reducing the delay from 50 to 20 fs results in a strong overlap of these pulses and the pulses become indistinguishable.

Figure 6c,d show the calculated (solid lines) first-order cross-correlation function of the SPP pulses from Figure 4a,b (see Supporting Information for details). As can be seen from Figure 4, the cross-correlation function allows determining the time delay between the pulses if the delay is much larger than the pulse duration. Indeed, as can be seen from the figure when the delay is equal to 50 fs, the two maxima appear in the cross-correlation function and the distance between them is 50 fs. Another picture is seen when the delay between pulses is comparable with the pulse duration and equals 20 fs. In the corresponding cross-correlation curve, these pulses are indistinguishable.

Figure 6c, d shows the measured results (black dots) of cross-correlation curves when SPPs are excited by a pair of laser pulses having 50 fs delay (Figure 6a) and 20 fs delay (Figure 6b). As can be seen from the presented data, the measured results (Figure 6c,d) are in good agreement with the calculations. These results convincingly demonstrate that two femtosecond SPP pulses with a time delay of Δt_1 = 50 fs are still distinguishable at a distance of 1 mm from the excitation region. This means that in such extra-long SPP focusing it is possible to transmit a pair of femtosecond SPP pulses with a distance between them equals 50 fs.

We presented in Figure 6 the measurements only for two fixed time delays between the laser and SPP pulses. We did the measurements also at other delays in the range from 20 to 100 fs (not presented here). Our measurements show that the 50 fs long delay between laser pulses is the minimum value at which the SPP waves (excited by the laser pulses) are time-resolved with the first-order cross correlation technique used. We note that this value correlates with our estimates on the limitations from the velocity dispersion of SPP waves. The minimal delay time between two pulses allows determining the frequency bandwidth of the investigated open-type SPP waveguide (see Supporting Information for details). Based on our measurements the amplitude modulation bandwidth equals 3.5 THz.

CONCLUSION

In this paper, we proposed and experimentally implemented a new type of waveguide in plasmonics, namely, an open-type SPP waveguide, based on the excitation of convergent SPP waves and their long distance focusing. In the SPP waveguide the transverse localization of the SPP waves is in a range 50−100 μm, but its effective propagation length is much larger than the propagation length of all known SPP waveguides. The demonstrated effective propagation length of SPP waves excited in an open-type SPP waveguide is 8× larger than the propagation length of the SPP waves on a bare Ag nanofilm surface.

One of the important applications of plasmonics is the transmission of information at a high speed. With the use of the open-type SPP waveguide, we considered the possibility of transmitting information by SPP waves over a distance equal to 1 mm. It was shown that the amplitude modulation of a focused SPP over a distance of 1 mm is characterized by a 3.5 THz bandwidth. The ultrafast dynamics of SPP waves were measured with the use of a first-order cross-correlation technique. Note that in plasmonics the possibility of information transfer over such a large distance is considered for the first time. The large effective propagation length of SPP waves in an open-type SPP waveguide and its ultrahigh bandwidth open up new possibilities of its use in different areas of plasmonics and photonics.

Another important application of an open-type SPP waveguide is its use for ultrasensitive detection. A broad spectrum of SPP waves excited in the waveguide and a long effective propagation length can help to realize a spectroscopy with a long interaction length, leading to establishing new records of sensitivity for SPP-based sensors.

ASSOCIATED CONTENT

Supporting Information

The Supporting Information is available free of charge on the ACS Publications website at DOI: 10.1021/acsphotonics.8b01787.

(1) Calculation of the SPP intensity distribution in the open-type SPP waveguide; (2) Estimation of SPP wave group velocity dispersion constraints upon SPP femtosecond pulse propagation; (3) Description of measurements of the open-type SPP waveguide bandwidth (PDF)

AUTHOR INFORMATION

Corresponding Author

*E-mail: melentiev@isan.troitsk.ru.

ORCID

Pavel N. Melentiev: 0000-0001-8958-453X

Funding

This work was supported by the Russian Foundation for Basic Research (Grant Nos. 17-02-01093 and 18-02-00315). The research was financially supported by the Advanced Research Foundation (Contract No. 7/004/2013−2018 on 23.12.2013). Sample fabrication was performed using equipment of MIPT Shared Facilities Center and with financial support from the Ministry of Education and Science of the Russian Federation (Grant No. RFMEFI59417 × 0014). V.V.K. appreciates financial support from the RNNU MEPhI program of the global competitiveness increase.

Notes

The authors declare no competing financial interest.

REFERENCES

(1) Ozbay, E. Plasmonics: merging photonics and electronics at nanoscale dimensions. *Science* **2006**, *311*, 189−193.

(2) Brongersma, M. L.; Shalaev, V. M. The case for plasmonics. *Science* **2010**, *328*, 440−441.

(3) Bozhevolnyi, S. I.; Khurgin, J. B. The case for quantum plasmonics. *Nat. Photonics* **2017**, *11*, 398−400.

(4) Zayats, A.; Smolyaninov, I.; Maradudin, A. Nano-optics of surface plasmon polaritons. *Phys. Rep.* **2005**, *408*, 131−314.

(5) Melentiev, P.; Balykin, V. Nano optical elements for surface plasmon waves. *Phys.-Usp.* **2019**, *62*, na.

(6) Khurgin, J.; Sun, G. In search of the elusive lossless metal. *Appl. Phys. Lett.* **2010**, *96*, 181102.

(7) Baburin, A.; Kalmykov, A.; Kirtaev, R.; Negrov, D.; Moskalev, D.; Ryzhikov, I.; Melentiev, P.; Rodionov, I.; Balykin, V. Toward theoretically limited SPP propagation length above two hundred microns on ultra-smooth silver surface. *Opt. Mater. Express* **2018**, *8*, 3254−3261.

DOI: 10.1021/acsphotonics.8b01787
ACS Photonics 2019, 6, 1425−1433

(8) Malureanu, R.; Lavrinenko, A. Ultra-thin films for plasmonics: a technology overview. *Nanotechnol. Rev.* **2015**, *4*, 259−275.
(9) Konopsky, V.; Alieva, E. Long-range propagation of plasmon polaritons in a thin metal film on a one-dimensional photonic crystal surface. *Phys. Rev. Lett.* **2006**, *97*, 253904.
(10) Grandidier, J.; des Francs, G.; Massenot, S.; Bouhelier, A.; Markey, L.; Weeber, J.-C.; Finot, C.; Dereux, A. Gain-assisted propagation in a plasmonic waveguide at telecom wavelength. *Nano Lett.* **2009**, *9*, 2935−2939.
(11) Bolger, P. M.; Dickson, W.; Krasavin, A. V.; et al. Amplified spontaneous emission of surface plasmon polaritons and limitations on the increase of their propagation length. *Opt. Lett.* **2010**, *35*, 1197−1199.
(12) Meng, X.; Liu, J.; Kildishev, A.; Shalaev, V. Highly directional spaser array for the red wavelength region. *Laser Photonics Rev.* **2014**, *8*, 896−903.
(13) Zhou, W.; Dridi, M.; Suh, J.; Kim, C.; Co, D.; Wasielewski, M.; Schatz, G.; Odom, T. Lasing action in strongly coupled plasmonic nanocavity arrays. *Nat. Nanotechnol.* **2013**, *8*, 506−511.
(14) Melentiev, P.; Kalmykov, A.; Gritchenko, A.; Afanasiev, A.; Balykin, V.; Baburin, S.; Ryzhova, E.; Filippov, I.; Rodionov, I.; Nechepurenko, I.; et al. Plasmonic nanolaser for intracavity spectroscopy and sensorics. *Appl. Phys. Lett.* **2017**, *111*, 213104.
(15) Maier, S. A.; Atwater, H. A. Plasmonics: Localization and guiding of electromagnetic energy in metal/dielectric structures. *J. Appl. Phys.* **2005**, *98*, 10.
(16) Krasavin, A.; Zayats, A. Passive photonic elements based on dielectric-loaded surface plasmon polariton waveguides. *Appl. Phys. Lett.* **2007**, *90*, 211101.
(17) Berini, P.; Charbonneau, R.; Lahoud, N.; Mattiussi, G. Characterization of long-range surface-plasmon-polariton waveguides. *J. Appl. Phys.* **2005**, *98*, No. 043109.
(18) Krenn, J.; Weeber, J. Surface plasmon polaritons in metal stripes and wires. *Philos. Trans. R. Soc., A* **2004**, *362*, 739−756.
(19) Maier, S.; Friedman, M.; Barclay, P.; Painter, O. Experimental demonstration of fiberaccessible metal nanoparticle plasmon waveguides for planar energy guiding and sensingSurface plasmon polaritons in metal stripes and wires. *Appl. Phys. Lett.* **2005**, *86*, No. 071103.
(20) Bozhevolnyi, S.; Volkov, V.; Devaux, E.; Ebbesen, T. Channel plasmon-polariton guiding by subwavelength metal grooves. *Phys. Rev. Lett.* **2005**, *95*, No. 046802.
(21) Bozhevolnyi, S.; Volkov, V.; Devaux, E.; Laluet, J.-Y.; Ebbesen, T. Channel plasmon subwavelength waveguide components including interferometers and ring resonators. *Nature* **2006**, *440*, 508.
(22) Bian, Y.; Zheng, Z.; Liu, Y.; Liu, J.; Zhu, J.; Zhou, T. Hybrid wedge plasmon polariton waveguide with good fabrication-error-tolerance for ultra-deep-subwavelength mode confinement. *Opt. Express* **2011**, *19*, 22417−22422.
(23) Grandidier, J.; Massenot, S.; Des Francs, G. C.; Bouhelier, A.; Weeber, J.-C.; Markey, L.; Dereux, A.; Renger, J.; González, M.; Quidant, R. Dielectric-loaded surface plasmon polariton waveguides: figures of merit and mode characterization by image and Fourier plane leakage microscopy. *Phys. Rev. B: Condens. Matter Mater. Phys.* **2008**, *78*, 245419.
(24) Melentiev, P.; Kuzin, A.; Balykin, V.; Ignatov, A.; Merzlikin, A. Dielectric-loaded plasmonic waveguide in the visible spectral range. *Laser Phys. Lett.* **2017**, *14*, 126201.
(25) Berini, P. Plasmon-polariton waves guided by thin lossy metal films of finite width: Bound modes of symmetric structures. *Phys. Rev. B: Condens. Matter Mater. Phys.* **2000**, *61*, 10484.
(26) Berini, P. Figures of merit for surface plasmon waveguides. *Opt. Express* **2006**, *14*, 13030−13042.
(27) De Leon, I.; Berini, P. Amplification of long-range surface plasmons by a dipolar gain medium. *Nat. Photonics* **2010**, *4*, 382.
(28) Andryieuski, A.; Zenin, V. A.; Malureanu, R.; Volkov, V. S.; Bozhevolnyi, S. I.; Lavrinenko, A. V. Direct characterization of plasmonic slot waveguides and nanocouplers. *Nano Lett.* **2014**, *14*, 3925−3929.
(29) Geisler, P.; Razinskas, G.; Krauss, E.; Wu, X.-F.; Rewitz, C.; Tuchscherer, P.; Goetz, S.; Huang, C.-B.; Brixner, T.; Hecht, B. Multimode plasmon excitation and in situ analysis in top-down fabricated nanocircuits. *Phys. Rev. Lett.* **2013**, *111*, 183901.
(30) Sun, C.; Rong, K.; Wang, Y.; Li, H.; Gong, Q.; Chen, J. Plasmonic ridge waveguides with deep-subwavelength outside-field confinements. *Nanotechnology* **2016**, *27*, No. 065501.
(31) Konopsky, V. N.; Alieva, E. V. Photonic crystal surface waves for optical biosensors. *Anal. Chem.* **2007**, *79*, 4729−4735.
(32) Fan, X.; White, I. M.; Shopova, S. I.; Zhu, H.; Suter, J. D.; Sun, Y. Photonic crystal surface waves for optical biosensors. *Anal. Chim. Acta* **2008**, *620*, 8−26.
(33) Prokhorov, A. M. Molecular amplifier and geterator for submillimeter waves. *J. Exp. Theor. Phys. (U.S.S.R.)* **1958**, *34*, 1658−1659.
(34) Schawlow, A. L.; Townes, C. H. Infrared and Optical Masers. *Phys. Rev.* **1958**, *112*, 1940−1949.
(35) Goubau, G.; Schwering, F. On the guided propagation of electromagnetic wave beams. *IRE Trans. Antennas Propag.* **1961**, *9*, 248−256.
(36) Weinstein, L. A. *Open Resonators and Open Waveguides*; Golem Press, 1969.
(37) Radko, I. P.; Bozhevolnyi, S. I.; Brucoli, G.; Martin-Moreno, L.; Garcia-Vidal, F. J.; Boltasseva, A. Efficient unidirectional ridge excitation of surface plasmons. *Opt. Express* **2009**, *17*, 7228−7232.
(38) Melentiev, P.; Kuzin, A.; Balykin, V. Control of SPP propagation and focusing through scattering from nanostructures. *Quantum Electron.* **2017**, *47*, 266−271.
(39) Melentiev, P. N.; Kuzin, A. A.; Negrov, D. V.; Balykin, V. I. Diffraction limited focusing of plasmonic wave by a parabolic mirror. *Plasmonics* **2018**, *13*, 2361−2367.
(40) Evlyukhin, A. B.; Bozhevolnyi, S. I.; Stepanov, A. L.; Kiyan, R.; Reinhardt, C.; Passinger, S.; Chichkov, B. N. Surface plasmon polariton beam focusing with parabolic nanoparticle chains. *Opt. Express* **2007**, *15*, 16667−166803.
(41) Kim, H.; Hahn, J.; Lee, B. Focusing properties of surface plasmon polariton floating dielectric lenses. *Opt. Express* **2008**, *16*, 3049−3057.
(42) Zhao, C.; Liu, Y.; Zhao, Y.; Fang, N.; Huang, T. J. A Reconfigurable Plasmofluidic Lens. *Nat. Commun.* **2013**, *4*, 2305.
(43) Ayata, M.; Fedoryshyn, Y.; Heni, W.; Baeuerle, B.; Josten, A.; Zahner, M.; Koch, U.; Salamin, Y.; Hoessbacher, C.; Haffner, C.; Elder, D.; Dalton, L.; Leuthold, J. Highspeed plasmonic modulator in a single metal layer. *Science* **2017**, *358*, 630−632.
(44) Kinsey, N.; Ferrera, M.; Shalaev, V.; Boltasseva, A. Examining nanophotonics for integrated hybrid systems: a review of plasmonic interconnects and modulators using traditional and alternative materials. *J. Opt. Soc. Am. B* **2015**, *32*, 121−142.
(45) Delacour, C.; Blaize, S.; Grosse, P.; Fedeli, J. M.; Bruyant, A.; Salas-Montiel, R.; Lerondel, G.; Chelnokov, A. E-cient directional coupling between silicon and copper plasmonic nanoslot waveguides: toward metal- oxide- silicon nanophotonics. *Nano Lett.* **2010**, *10*, 2922−2926.
(46) Lee, H. W.; Papadakis, G.; Burgos, S. P.; Chander, K.; Kriesch, A.; Pala, R.; Peschel, U.; Atwater, H. A. Nanoscale conducting oxide PlasMOStor. *Nano Lett.* **2014**, *14*, 6463−6468.
(47) Nielsen, M. P.; Shi, X.; Dichtl, P.; Maier, S. A.; Oulton, R. F. Giant nonlinear response at a plasmonic nanofocus drives efficient four-wave mixing. *Science* **2017**, *358*, 1179−1181.
(48) Matsumoto, M.; Tsutsumi, M.; Kumagai, N. Bragg reflection characteristics of millimeter waves in a periodically plasma-induced semiconductor waveguide. *IEEE Trans. Microwave Theory Tech.* **1986**, *34*, 406−411.
(49) Saadoun, M.; Engheta, N. A reciprocal phase shifter using novel pseudochiral or Ω medium. *Microwave and optical technology letters* **1992**, *5*, 184−188.
(50) Klimov, V. *Nanoplasmonics*; Pan Stanford Publishing, 2014.

DOI: 10.1021/acsphotonics.8b01787
ACS Photonics 2019, 6, 1425−1433

(51) McPeak, K. M.; Jayanti, S. V.; Kress, S. J.; Meyer, S.; Iotti, S.; Rossinelli, A.; Norris, D. J. Plasmonic films can easily be better: rules and recipes. *ACS Photonics* **2015**, *2*, 326−333.
(52) Kuttge, M.; García de Abajo, F.; Polman, A. How grooves reflect and confine surface plasmon polaritons. *Opt. Express* **2009**, *17*, 10385−10392.
(53) Lemke, C.; Schneider, C.; Leiner, T.; Bayer, D.; Radke, J.; Fischer, A.; Melchior, P.; Evlyukhin, A.; Chichkov, B.; Reinhardt, C.; Bauer, M.; Aeschlimann, M. Spatiotemporal characterization of SPP pulse propagation in two-dimensional plasmonic focusing devicess. *Nano Lett.* **2013**, *13*, 1053.

DOI: 10.1021/acsphotonics.8b01787
ACS Photonics 2019, 6, 1425−1433